Available online at www.eccomasproceedia.org
Eccomas Proceedia COMPDYN (2023) 3203-3212

ECCOMAS
Proceedia

COMPDYN 2023
9th ECCOMAS Thematic Conference on
Computational Methods in Structural Dynamics and Earthquake Engineering
M. Papadrakakis, M. Fragiadakis (eds.)
Athens, Greece, 12-14 June 2023

TIMBER CARPENTRY WITHOUT STEEL CONNECTORS

Luigi Massaro[1], Roberto Serpieri[1], Giorgio Frunzio[1] and Luciana Di Gennaro[1]

[1] Department of Architecture and Industrial Design, University of Campania Luigi Vanvitelli
81033, Aversa, Italy
{luigi.massaro, roberto.serpieri, giorgio.frunzio, luciana.digennaro}@unicampania.it

Abstract

Use in modern timber constructions of wood-wood connections inspired by traditional timber carpentry can take advantage today of the many available digital technologies aiding stress analysis and automated control of machining tools. Such methodologies of more recent introduction, if properly employed, allow for a reduction in time and of human error in the design and manufacturing phases of timber structures. Wood-wood connections without metal elements are encountered in many historical buildings. However, not infrequently in intervention on existing timber elements as well as in new timber constructions, the original connection typologies are renounced in favor of other connection typologies due to higher costs and the difficulty of thoroughly analyzing the structural behaviour of wood-only joints under the full set of loading conditions and design seismic actions prescribed by the building regulations currently in force. The connection typologies between timber elements may differ according to the loading types (stress-resultant) for which they are designed to. The most common are carpentry joints and mechanical joints. The former is the traditional union of timber carpentry using woodworking of contacting surfaces. Mechanical joints provide, instead, for the use of metal connections and/or glue layers. Fostering the use of wood-wood connections brings several advantages: (i) exploring the value of timber-timber connections as an ancient cultural heritage amenable to provide methodologies suitably implementable in the design processes of the modern construction industry, with a specific view towards the rehabilitation of historical and monumental buildings; (ii) understanding by parametric computer-aided analyses, in desirable retracing of the past rules of the art, the influence of wood fiber orientation also in the use of engineered composite timber assemblies like CLT; (iii) foster the use of local wood; (iv) measure the fire-resistance of timber joints. This contribution has the twofold purpose of summarizing the state-of-the-art in the structural design of a wood carpentry joint in absence of strengthening metal connectors and exploring the possibilities offered by an ad-hoc stress analysis software for the parametric finite-element analysis of timber joints.

Keywords: connections, timber, CLT, existing structures, design processes.

ISSN:2623-3347 Published by Eccomas Proceedia.
Peer-review under responsibility of the organizing committee of COMPDYN 2023.
doi: 10.7712/120123.10633.20422

1 INTRODUCTION

Several economic and technological factors recently brought into prominence in Italy, also caused by geopolitical processes of larger geographical and temporal scales, ultimately traceable to ecological and environmental problems [1,2], suggest today a more conscious reconsideration of timber as building construction material in civil engineering. Wood has always been used as a building material and, thanks to its characteristics, it responds well to current environmental needs [1–3]. This applies both to solid wood and engineered woods such as glued laminated timber (GLT) and cross-laminated timber (CLT). The latter has been widely used in recent decades both for interventions on existing structures [4] and for the construction of new buildings. The connections between the wooden elements play a key role in the intervention's stability. Selective use of wood-wood connections without metal elements can be found in many historical buildings and bridges [5–7]. This suggests analyzing the connection of wood elements without the use of steel connectors.

In the Campania area in southern Italy, an example of wooden structures of monumental historical value is the roof in solid chestnut wood covering the local warehouse and storage building of the Cemetery of Santa Maria del Popolo (known as the cemetery of the 366 pits), designed by Ferdinando Fuga in the second half of the '700 [8] and located in Naples in the Poggioreale district (Fig.1).

Figure 1: Chestnut truss of the roof of the Cimitero delle 366 fosse, Naples.

Still in the Campania area, an example of renovation in GLT, of the roof of a historic structure, is the relatively recent replacement of the trusses of the graduation hall at the Faculty of Architecture of the University of Campania "Luigi Vanvitelli", within the monastery complex of San Lorenzo "ad Septimum" in Aversa (Fig.2).

Figure 2: GLT roof truss in Monastery complex of Lorenzo ad Septimum, Aversa.

The monastery, founded around the year one thousand by the Benedictines and located on the Roman consular road near Capua, became with the Normans one of the most important abbeys in southern Italy and was subsequently used as a military school, a military orphanage, and later as institute of art and mechanics, as well as for other educational activities [9,10].

In this contribution, a computational study is presented addressing structural analyses accounting for dynamic loads for a future replacement in solid wood of the trusses of San Lorenzo's roof, without using glues or metal connectors. Such a research problem is identified as a relevant one, proceeding from the consideration that it can be of general interest for interventions of sustainable renovation of the wooden roofing structures of many buildings of historical and monumental importance both of sacred and civil architecture [11]. Special attention is devoted herein to the analysis of the central connection between the kingpost and left and right struts by questioning the capability of this joint to sustain seismic loads avoiding exit of the struts' lower ends from the notched saddle supports in absence of metallic restraints or glues. Details of these notched saddles are shown in Fig.3a, which is an enlargement of the bottom connections of Fig.2, and in Fig.3b showing similar notched supports in the wooden trusses of the roof of the Church of the Nativity in Bethlehem [12,13].

a)

b)

Figure 3: Detail of notched saddle supports in kingpost-struts connections. a), enlargement from Fig.2; b), detail from the Church of the Nativity in Bethlehem.

Computational analyses were carried out employing the finite-element code for static and environmental sustainability of structures: MORES (Multipurpose Object-oriented Research Environment for Structures).

Section 2 introduces a few selected aspects concerning the approach to structural and computational analysis of wood-wood connections. In Sect. 3, the truss structure is described, and a design problem is presented relevant to the response to dynamic loads of the connection between kingpost and struts, together with some numerical results.

2 WOOD-WOOD JOINTS IN DYNAMIC STRUCTURAL ANALYSIS

Wood has long been used for building structurally connected assemblies subjected to dynamic loading, an example of which can be the *capra*, an ancient Roman machinery which, according to some authors, may have been at the very origin of the Italian name *capriata* for timber roof truss. The capability of timber to reliably sustain dynamic loads is also testified by its ordinary employment, at the beginning of the past century, as a construction material for manufacturing specific structural components in aircraft engineering [14]. In the field of building constructions, where wood is frequently employed for roofing systems, the treatise of Architecture by Sebastiano Serlio [6] remarked on the importance of duly considering the dynamic action of wind loads for selecting

the proper structural typology and dimension of roof truss structures. Book VII of this treatise illustrates, in particular, several wood joint typologies, many of which, at selected connection sites of specific truss typologies, are constructed without any use of nails and steel reinforcements [6]. This category of joints, where connection can be guaranteed solely by friction and interlocking between the contacting wooden surfaces, are denominated carpentry joints. On the opposite side are mechanical joints where stress transmission is ensured by other non-ligneous materials or devices such as glue, metallic connectors and/or restraints including ropes. Some typologies of carpentry joints are exemplified in Fig.4.

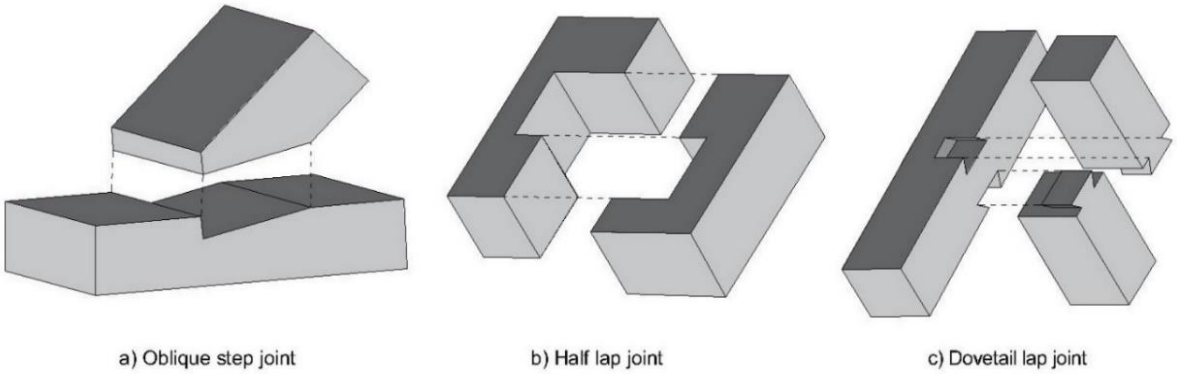

Figure 4: Some traditional typologies of carpentry joints.

Computational stress analysis of wood connections cannot rule out the orthotropic features of timber, given the considerable difference – usually even higher than a tenfold factor – of strength and stiffness between values attained in grain direction and orthogonal to grain direction [15,16].

The mechanical characteristics of wood strongly vary between conifers and deciduous trees and often even between individual trees of the same species. In general, in a tree, most of the wood-cells are elongated, like a hollow cylinder oriented along the axis of the trunk. The residual ones are arranged in radial direction. By virtue of these considerations, wood can be seen as a material having at any point three perpendicular planes of elastic symmetry, identified by three axes. Herein, as shown in Fig.5, L is the grain direction, R the radial direction, while T is orthogonal to L and R.

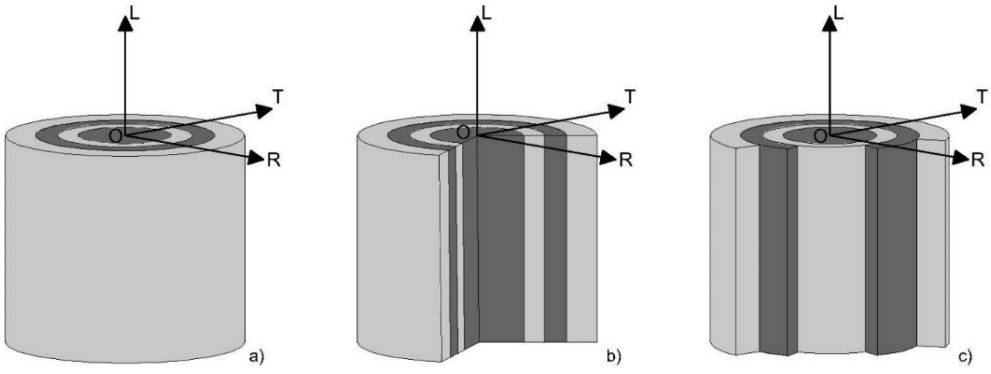

Figure 5: Reference system based on wood nature.

The computational analyses in this study employ frame-element models and 2D plane-stress membrane models. In the latter, transverse isotropy is assumed as an approximation acceptable to the benefit of simplicity in setting input parameters, thus treating directions T and R as identical from the mechanic point of view. Working in a reference frame x_1x_2 of axes of transverse-isotropy coinciding with plane-stress membrane axes (with axis x_1 being aligned to OL), plane-stress elastic relations admit in Voigt notation the following representation:

$$\{\sigma\} = [K]\{\varepsilon\}: \qquad \begin{Bmatrix} \sigma_{x_1} \\ \sigma_{x_2} \\ \tau_{x_1x_2} \end{Bmatrix} = \begin{bmatrix} \frac{E_1}{1-\nu_{12}\nu_{21}} & \frac{E_1\nu_{21}}{1-\nu_{12}\nu_{21}} & 0 \\ \frac{E_2\nu_{12}}{1-\nu_{12}\nu_{21}} & \frac{E_2}{1-\nu_{12}\nu_{21}} & 0 \\ 0 & 0 & 2G_{12} \end{bmatrix} \begin{Bmatrix} \varepsilon_{x_1} \\ \varepsilon_{x_2} \\ \gamma_{x_1x_2}/2 \end{Bmatrix} \tag{1}$$

where the usual notation for orthotropy is employed to denote Young moduli E_1, E_2, the shear modulus G_{12} and Poisson ratios ν_{12}, ν_{21}, and where, in compliance with transverse isotropy, the constraint $\nu_{21}E_1 = \nu_{12}E_2$ must hold.
In modeling connections among wood frames of different direction by 2D plane-stress membrane models, coordinates changes become necessary. The usual formula giving components-change of a fourth-order tensor c_{ijhk} as a consequence of a rotational change of reference axes directions $x_1x_2x_3 \longrightarrow x_1,x_2,x_3,$ (defined by the orthonormal 3×3 one-covariant and one-contravariant tensor Q_{ij}), reading $c'_{ijhk} = Q_{li}\, Q_{mj}Q_{ph}Q_{qk}c_{lmpq}$, achieves, by virtue of the hypotheses and notational conventions above and of minor and major symmetries of the elastic tensor, the following simpler representation in Voigt matrix format

$$[K]' = \left[M_Q\right][K]\left[M_Q\right]^{-1}, \tag{2}$$

where $\left[M_Q\right]$ is a matrix, associated with an in-plane rotation by an angle ϑ, defined as:

$$\left[M_Q\right] = \begin{bmatrix} \cos^2\vartheta & \sin^2\vartheta & 2\cdot\sin\theta\cos\theta \\ \sin^2\vartheta & \cos^2\vartheta & -2\cdot\sin\theta\cos\theta \\ -\sin\theta\cos\theta & \sin\theta\cos\theta & \cos^2\vartheta - \sin^2\vartheta \end{bmatrix}. \tag{3}$$

The properties of the wood material considered in the analyses of the following section are calibrated upon chestnut (Castanea sativa). This choice stems from the copious presence of chestnut elements in many structures and historic buildings, especially in southern Italy. References for these values are taken from [14,17–20] and summarized in Table 1.

Wood Species	density [Kg/mc]	moisture [%]	E [GPa]
Chestnut	508	12	13,8

Table 1: Properties of chestnut and walnut.

3 NUMERICAL ANALYSIS OF A WOOD-WOOD TIMBER ROOF TRUSS JOINT

The structural analyses reported in this section examine a replacement in solid chestnut of the wood truss sustaining the roof of the graduation hall within the monastery complex of San Lorenzo ad Septimum in Aversa. The truss typology is an *Italian capriata* with kingpost-struts joint – in Italian technical nomenclature termed *giunto monaco-saette* and hereafter referred to in brief as KS joint – statically unconnected from the horizontal *catena*, conforming to the classical static scheme and carpentry details already documented by Luciano da San Gallo and retraceable to the ancient Roman empire, since already present in the original paleo Christian Basilica of San Paolo fuori le Mura [5]. In such scheme the lower catena element is conveniently exempt from flexural loads, except for those originated by self-weight, thus acting as a pure tie.
The span as well as the characteristic dimensions and carpentry joint details considered in the analyses are dimensioned upon those of the currently existing GLT structure. Span and height are approximately 12.0 m and 3.2 meters. Fig.6 shows the single-line frame-assembly 2D scheme with constraints employed in frame analyses. In the structural analyses herein presented, left and right struts are modelled as elements bearing only axial force, by addition of terminal hinges, assuming rotational capacity granted by the notched saddles visible in Fig.3 left and sketched in Fig.7 with geometrical details. Roof struts AC and CB are continuous. Bearing B was modeled both as a simple

support, to gain insight into the stress on the tie A-B, and as a as complete external hinge, to obtain a symmetric model.

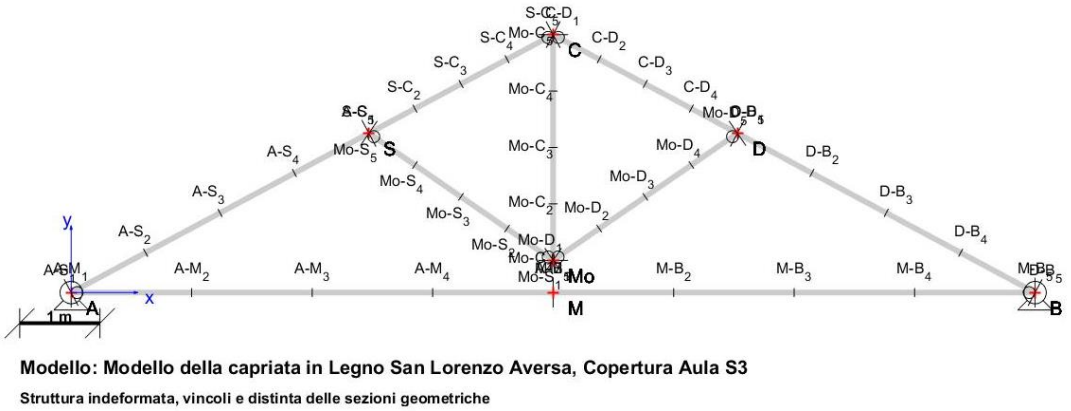

Figure 6: **S**ingle-line frame-assembly diagram with constraints of San Lorenzo's roof truss structure.

Kingpost and struts have section 24x24 cm, roof struts are 24x30 cm, while the tie is 24x40 cm.
A front-planar sketch of the KS joint with relevant dimensions and carving angles is shown in Fig.7.

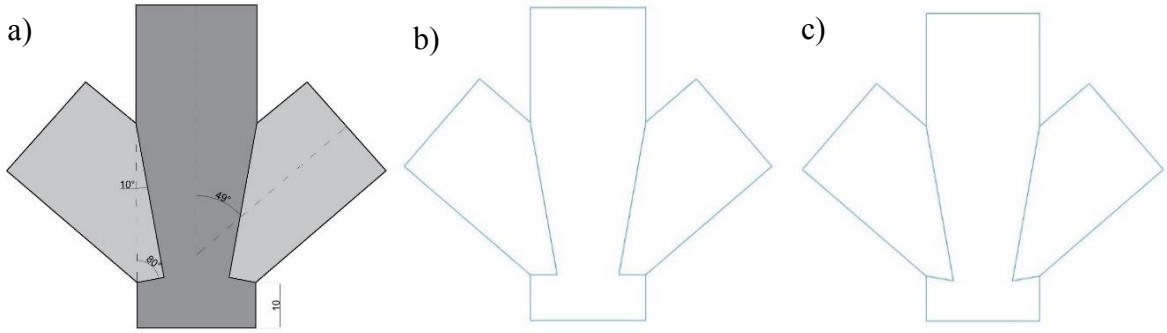

Figure 7: Detail sketch of the analyzed geometries for the KS joint with dimensions of carving angles. In all sketches upper carving angles are 10° while lower carving angles are: a) 80°; b) 90°; c) 100°.

Response of this structure to dynamic loads is investigated by examining the capability of the KS joint to resist seismic loads while preventing, even in complete absence of metallic restraints or glues, the struts falling off the notched saddle supports at the lower end of the kingpost element.

Computer-aided stress analyses were carried out employing frame and plane-stress membrane finite-element models within the multi-criteria object-oriented code MORES for static and environmental sustainability of structures. A first beta version of this code has been developed and benchmarked in Matlab® at the Department of Architecture of the University of Campania as an open-source multiplatform project.

From pre-dimensioning, dynamic loads which are found significant for the potential activation of such a collapse mechanism are identified only in seismic loads, since dimensioning of wind loads based upon NTC 2018 section 3.3 [21] – leads to much lower and negligible actions. The gravity load (1,700 kN), the horizontal seismic load (210 kN) and the vertical seismic load (105 kN), were essentially determined based on NTC 2018 [22], and are modeled as distributed forces over the roof struts. Fig.8 shows the four elementary load cases considered in the analyses: a) gravity load, b) horizontal seismic load, c) vertical seismic load, d) seismic asynchronous oscillation of roof pitches. The fourth load case is contemplated proceeding from considerations about structural and loading symmetries. In the symmetric scheme with hinges in both A and B, the KS joint remains unloaded

when subjected to load case b) alone, since this load case constitutes an antisymmetric loading distribution over a structure which is both geometrically symmetric and symmetrically constrained. Such symmetries, and the property of the kingpost tie of being only amenable to symmetric centered axial loads and located above the symmetry axis and located over the symmetry axis, bring the consequence that the KS joint remains unloaded under full-span horizontal seismic loading which is antisymmetric. Load case d) was consequently included among the elementary cases to be combined, referred to a hypothetical asynchronous horizontal movement of one pitch possibly originated by backlash between the left and right frames of the truss.

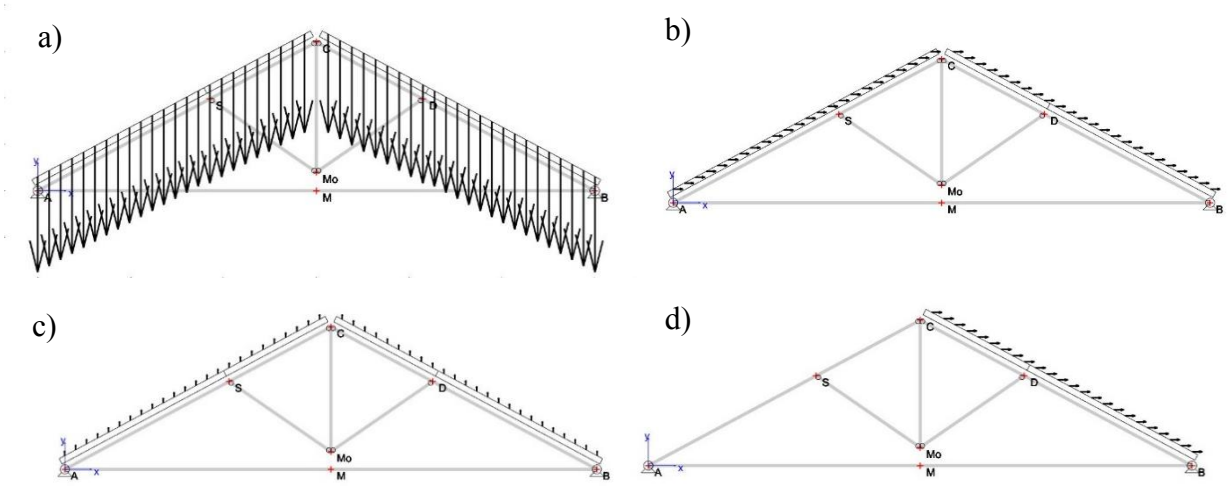

Figure 8: Elementary load cases considered: a) gravity load, b) horizontal seismic load, c) vertical seismic load d) seismic asynchronous oscillation. Representation of distributed loads are in scale.

The response of the KS joint to dynamic loading has been also investigated by 2D plane-stress finite-element membrane hierarchical sub-models, providing detailed analyses of the joint connections of the primary frame-element model. The 2D mesh consists of the structured hierarchical mesh of Constant Stress Triangles (CST) [23] shown in Fig.9a. Prior to its use, the element implementation was benchmarked based on analytical solutions of isotropic and transversely isotropic beams by also exploiting the closed-form analytical solution with full account of shear deformability and shear principal axes originally proposed in [24] . The structure is supported at the upper kingpost cross section and forces acting on struts' cross sections are hierarchically determined. The joint is modeled assuming, as first-step condition, perfect bilaterally contacting surfaces.

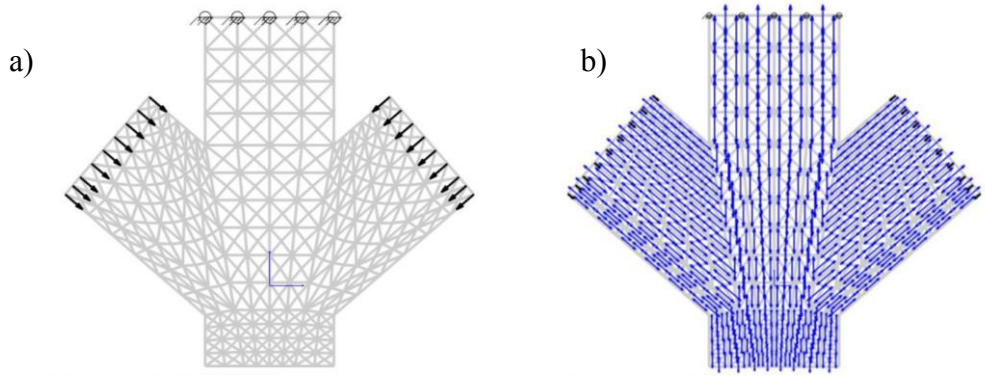

Figure 9: KS finite-element model: a) employed mesh; b) grain directions.

Different grain orientations in the three membrane subparts are shown in Fig.9b and are computationally addressed as described in the previous section.

4 RESULTS AND CONCLUSION

Fig.10 illustrates a selection of moment diagrams and axial force diagrams associated with some of the elementary load cases of Fig.8 for the symmetric and unsymmetric constraint schemes. In particular, Fig.10a shows, for the symmetric scheme with two external hinges, the function of struts in creating an intermediate support reducing span, maximum moment and deflection in struts AC ed CB. For the same constraint scheme, Fig.10b shows that the KS joint remains unloaded under full-span horizontal loads since this load case constitutes an antisymmetric loading distribution over a structure which is both geometrically symmetric and symmetrically constrained. Fig.10c illustrates the response in the unsymmetric simply supported scheme, with linear variation of axial force in AC and BC due to the longitudinal component of distributed horizontal load, and with the function exerted by the horizontal tie in preventing external transfer of horizontal loads to the bearing structure. Fig.10d shows the elementary demand of axial tensile type over the struts for the seismic half-span loading.

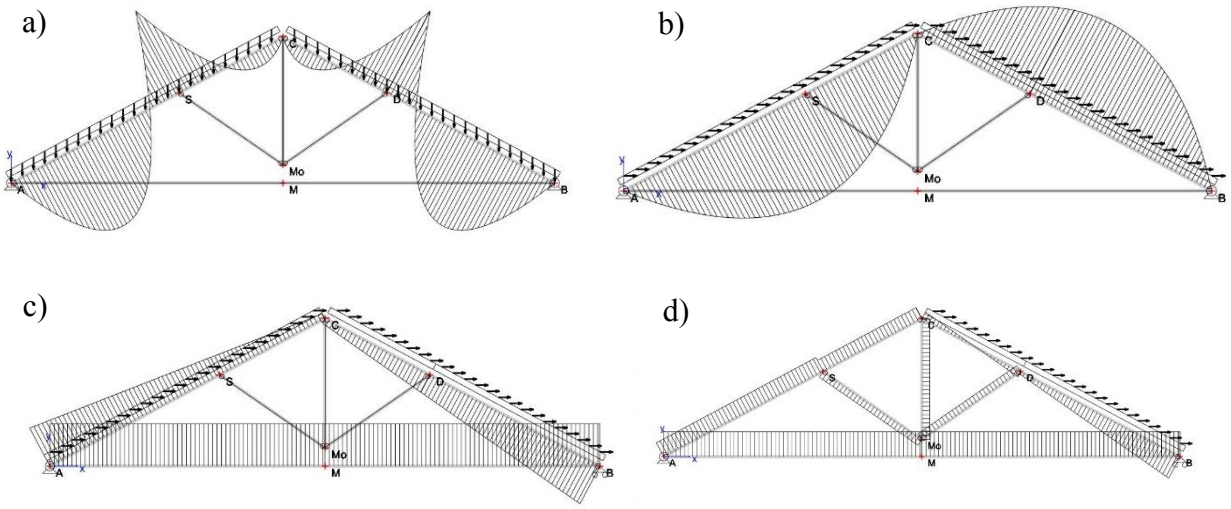

Figure 10: a) Moment diagrams with complete external hinges at both bearings (gravitational load case); b) Moment diagrams with complete external hinges at both bearings (seismic full-span load case); c) Axial load diagrams in the unsymmetric scheme with hinge on the left and simple support on the right (seismic full-span load case; d) Axial load diagrams in the unsymmetric scheme with hinge on the left and simple support on the right (seismic half-span). Scale factors of diagrams are not the same in figures.

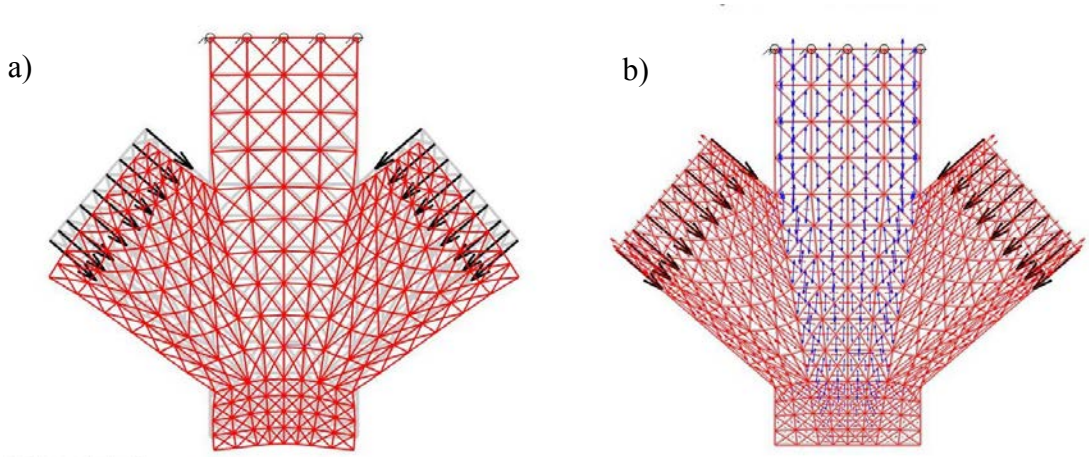

Figure 11: KS finite-element model: a) deformed mesh (displacements magnified by a factor **10** ×; b) principal stresses (tensile stresses in blue, compressive stresses in red).

Stress-resultant actions across node 'Mo' contributed by elementary load cases have been used, upon suitable linear combination, as input loading demands for determining the static performance of this node by higher-detail 2D membrane models of the typology exemplified in Fig.9. A deformed mesh and principal stresses for a 2D analysis for the purely gravitational load case are shown in Fig.11.

Altogether, the computer-aided finite-element analyses have shown the capability of the KS joint to sustain seismic loads avoiding exit of the struts' lower ends from the notched saddle supports with no appearance of tensile stresses over contacting surfaces and in absence of any supplemental non-wood bilateral restraints. Such result would show that – at least as far as the modelling hypotheses herein assumed for interaction of elementary frames, loading, mechanical contact, and geometry are concerned – it is possible to construct the KS joint according to the 'rules of the art' and sustain dynamic loads without metal connectors or glues.

Future lines of research departing from this study will address nonlinear contact, friction and explore minimum-maximum problems for optimal selection of materials, joint details and structural schemes, in a perspective of sustainability.

REFERENCES

[1] *Kyoto Protocol to the United Nations Framework Convention on Climate Change*, 2303 U.N.T.S., 1997.

[2] United Nations General Assembly, United Nations, The 2030 Agenda and the Sustainable Development Goals, 2015.

[3] *Legge 28 dicembre 2015, n. 221 - Disposizioni in materia ambientale per promuovere misure di green economy e per il contenimento dell'uso eccessivo di risorse naturali.*

[4] G. Frunzio, S. Rinaldi, M. Guadagnuolo, L. Massaro, and L. di Gennaro, "Use of engineered wood for the retrofitting of existing structures," in *9th International conference on harmonisation between architecture and nature - Eco-Architecture 2022*, 2022.

[5] S. Valeriani, "Monaci, dardi e colonnelli: genesi e caratteristiche delle capriate italiane," 2005.

[6] S. Serlio, *Il settimo libro d'Architettura*, Francesco de' Franceschi, 1600.

[7] G. da Sangallo and C. Hülsen, *Il libro di Giuliano da Sangallo: Codice vaticano barberiniano latino 4424*, Biblioteca apostolica vaticana, 1984.

[8] P. Giordano, "Il restauro e la riconfigurazione architettonica del Cimitero delle 366 Fosse e del Sepolcreto dei Colerici a Napoli," *Festival dell'Architettura Magazine*, 42–49, Festival Architettura Edizioni, 2021.

[9] L. Santagata, "Storia di Aversa", Eve Editrice, 1991.

[10] L. Santagata, "Storia di Aversa", Eve Editrice, 1991.

[11] G. Frunzio and L. di Gennaro, "Seismic structural upgrade of historical buildings through wooden deckings strengthening: The case of study of Palazzo Ducale in Parete, Italy," *Procedia Structural Integrity* **11**, 153–160, Elsevier B.V., 2018.

[12] C. Alessandri, V. Mallardo, B. Pizzo, and E. Ruocco, "The roof of the Church of the Nativity in Bethlehem: Structural problems and intervention techniques," *Journal of Cultural Heritage* **13**, e70–e81, Elsevier Masson SAS, 2012.

[13] G. Faella, G. Frunzio, M. Guadagnuolo, A. Donadio, and L. Ferri, "The Church of the Nativity in Bethlehem: Non-destructive tests for the structural knowledge," *Journal of Cultural Heritage* **13**, e27–e41, Elsevier Masson SAS, 2012.

[14] C. F. Jenkin, “Report on materials of construction used in aircraft and aircraft engines,” 1920.

[15] J. Bodig and B. A. Jayne, “Mechanics of wood and wood composites,” 712, Van Nostrand Reinhold, 1982.

[16] A. T. Price, “A mathematical discussion on the structure of wood in relation to its elastic properties,” *Philosophical Transactions of the Royal Society of London. Series A, Containing Papers of a Mathematical or Physical Character* **228**, 1–62, 1929.

[17] M. Nocetti, M. Brunetti, and M. Bacher, “Efficiency of the machine grading of chestnut structural timber: prediction of strength classes by dry and wet measurements,” *Materials and Structures/Materiaux et Constructions* **49**, 4439–4450, Kluwer Academic Publishers, 2016.

[18] M. Brunetti, M. Nocetti, and P. Burato, “Strength Properties of Chestnut Structural Timber with Wane,” *Adv Mat Res* **778**, 377–384, Trans Tech Publications Ltd, 2013.

[19] M. Nocetti, M. Bacher, S. Berti, M. Brunetti, and P. Burato, “Machine Grading of Chestnut Structural Timber with Wane,” 2013.

[20] M. Nocetti, M. Bacher, M. Brunetti, A. Crivellaro, and J.-W. G. van de Kuilen, “Machine grading of Italian structural timber: preliminary results on different wood species,” 2010.

[21] D. Min. Infrastrutture e Trasporti 17gennaio 2018, *Norme tecniche per le costruzioni (NTC 2018), paragrafo 3.3 Azioni del vento - (Technical standards for construction - section 3.3. wind actions)*, 2018.

[22] D. Min. Infrastrutture e Trasporti 17gennaio 2018, *NTC 2018 - Norme tecniche per le costruzioni. (Technical standards for construction),* 2018.

[23] N. Carpenter, H. Stolarski, and T. Belytschko, “Improvements in 3-node triangular shell elements,” *Int J Numer Methods Eng* **23**, 1643–1667, 1986.

[24] R. Serpieri, “On the Equivalence of Energetic and Geometric Shear Factors Based on Saint Venant Flexure,” *J Elast* **116**, 115–160, 2014.